

MODELLING CHANGES IN THE GLOBAL METHANE HYDRATE INVENTORY

Stephen Hunter* and Alan Haywood
School of Earth and Environment,
University of Leeds
Leeds, LS2 9JT
UNITED KINGDOM

Denis Goldobin, Nikolai Brilliantov and Jeremy Levesley
Department of Mathematics,
University of Leicester
Leicester, LE1 7RH
UNITED KINGDOM

John Rees, Peter Jackson, Chris Rochelle and Mike Lovell
British Geological Survey
Keyworth
Nottingham, NG12 5GG
UNITED KINGDOM

Andy Ridgwell
School of Geographical Sciences
University of Bristol
Bristol, BS8 1TH

ABSTRACT

We present results from a study designed to investigate how the global methane hydrate reservoir has changed through the last glacial-interglacial cycle. Bottom water conditions are derived from a series of long-integration snapshot-type HadCM3 GCM experiments that cover the last 120 kyr. We use this dataset to drive a 1D transient hydrate model. We first evaluate the model using sensitivity experiments against a number of hydrate bearing ODP/DSDP sites. We then explore potential initial and final steady-state inventories using Pliocene and modern boundary conditions and compare to previous studies. We then investigate how the potential volume of submarine hydrate has evolved from initial Pliocene conditions through a series of pseudo glacial cycle. We find that the potential volume increases from $7.3 \times 10^6 \text{ km}^3$ during the Pliocene to between 7.95 and $8.10 \times 10^6 \text{ km}^3$ during the last glacial cycle. Finally, we use our transient hydrate model, within a series of sensitivity studies, to investigate how the evolution of this potential volume is occupied by hydrate.

Keywords: methane hydrates, submarine hydrates, HadCM3, transient model

* Corresponding author: Phone: +44 Fax +44 E-mail: S.HUNTER@leeds.ac.uk

NOMENCLATURE

BHSZ Base of the Hydrate Stability Zone
EPICA European Project for Ice Coring in Antarctica
HadCM3 Hadley Centre Climate Model 3
HSZ Hydrate Stability Zone
GCM General Circulation Model
LHS Latin-Hypercube Sampled
LGM Last Glacial Maximum (23-19 ka)
MPWP mid-Pliocene Warm Period
PETM Paleocene-Eocene Thermal Maximum
PMIP Paleoclimate Modeling Intercomparison Project

G Geothermal gradient (K/m),
 rxn rate constant for methanogenesis (1×10^{-13} s)
 P porosity (unitless)
 sed Sedimentation Rate (cm/kyr)
 TOC Total Organic Carbon (wt %)
 $velup$, Interstitial fluid velocity at base (mm/yr)

INTRODUCTION

Methane hydrates present a potential hazard under anthropogenic climate change. The sensitivity of hydrate stability to changes in local pressure-temperature conditions and their existence beneath relatively shallow marine environments, mean that submarine hydrates are vulnerable to changes in bottom water conditions (i.e. warming).

The potential climate impact of methane release following dissociation of hydrate has in the past been compared to climate feedbacks associated with the terrestrial biosphere and identified as a possible trigger of abrupt climate change. Support for the role of methane hydrate in terrestrial and marine records is extensive. Examples include the PETM thermal maximum [1,2,3] and during Deglacial stages (including the termination of the Younger Dryas [4] and limiting the extent of glaciation [5,6]), although further work is required to fully understand these records. The role of hydrate disassociation as a trigger for submarine landslides has also been questioned and investigated [1,7,8,9,10], with reports of known hydrate occurrences that coincide with slumping and submarine landslides are common [9,10,11]. It is therefore imperative to improve our understanding of the global hydrate inventory and how it has changed in the past, so that we can begin to develop a picture of how it may change under anthropogenic climate change.

EXPERIMENT DESIGN

Our goal is to model the evolution of the global submarine methane hydrate inventory through the last glacial-cycle, so that we can begin to understand how it may change under future climate change.

We implement the time-dependent hydrate model of Davie, M.K. and B.A. Buffett., (2001) [12,13], evaluate a re-coded version against ODP-DSDP sites, adapt the model to make it fully transient (changing input conditions), and then apply the model to a pseudo-glacial cycle time-series, initialised with Pliocene boundary conditions.

We acknowledge that many required fields over the global domain are poorly-known or consist of a geographically-sparse data, particularly concerning temporal resolution. This project therefore aims to develop an initial first-order evaluation of the temporal evolution of the HSZ and hydrate inventory.

HadCM3 climate model

An in-depth description of the HadCM3 model used in this study can be found within [15]. The model was developed at the Hadley Centre for Climate Prediction and Research, part of the UK Meteorological Office, and is one of the first to be developed without the requirement for heat and salinity flux-adjustments [14]. The GCM consists of coupled atmosphere, ocean and sea-ice components [15]. The resolution of the ocean model is $1.25^\circ \times 1.25^\circ$ with 20 vertical levels in a geopotential co-ordinate system. The ocean physics are described within [15], and its performance has been explored within [16]. The climate model was used within the IPCC 3rd and 4th assessment reports [17] and the PMIP2 study [18]. HadCM3 and its model components have been used successfully in a number of Quaternary [19,20] and pre-Quaternary [21,22,23,24] modelling studies.

The series of long-integration HadCM3 GCM experiments covering the glacial-interglacial period are described fully within [25]. Orbital parameters are taken from [26]. Atmospheric composition is derived from ice-core, with CO₂ levels from the Vostok record [27,28] whilst CH₄

and NO_2 are derived from the EPICA record [29]. Post-LGM ice-sheet configurations are derived from the ICE5G reconstruction of [30] whilst pre-LGM configurations are derived from [31]. Ice sheet areal extent and thickness during interglacial to LGM times is scaled from the LGM ICE5G ice sheet reconstruction and linearly regressed using the SPECMAP $\delta^{18}\text{O}$ record of [32]. Sea level is derived from [31].

62 experiments cover the period from the Last Interglacial (120 kyr BP) to the present day. From 120 to 80 kyr BP an experiment is conducted every 4 kyr, from 80 to 20 kyr BP every 2 kyr and from 21 to 0 kyr BP every 1 kyr. All experiments are initialised from the same preindustrial climatology and run for 700 years. Bottom water conditions (temperature and salinity) were derived from the last 30 model years. The model integration was considered sufficiently long so as to give bottom water conditions, particularly in the margins, a chance to reach equilibrium. Whilst the study of [33] dismissed the HadCM3 model on the grounds that satisfactory levels of bottom water equilibrium were not attained, this study relies upon longer integration times. Nevertheless, whilst not all the ocean floor has reached equilibrium (for discussion see [16], a satisfactory equilibrium state is achieved for the continental margins where hydrates are likely to reside.

1-D transient hydrate model

Our hydrate model is a re-coded version (from Matlab™ to Fortran 90) of the time-dependent 1-D hydrate model of [12,13]. It is designed to model stratigraphic hydrate accumulations over geological-timescales. Modifications to the code have been made to make some calculations more efficient, this has resulted in the model being at least an order of magnitude quicker than the original code whilst running at higher vertical resolution. We have made alterations to the standard code to account for changing boundary conditions. We make the assumption of a methane-only system (i.e. no higher hydrocarbons) and fix salinity at 35 psu. The sulphate-reduction zone is specified as a fixed boundary condition within which methane is depleted. The BHSZ is determined through minimization of $T(z)-T_3$ where T_3 is calculated with the assumption that $P(z)$ is P_3 , therefore we find the depth bin which closely corresponds to $T_3(P)$. The vertical domain is set to $2 \times$ BHSZ. Calculation of BHSZ is generally

achieved to within 0.1 to 0.2m depending upon the vertical resolution, water depth, and BWT. The down-column equilibrium methane concentration takes an exponential form from 0 at the sea-floor, to a value determined by Henry's law at and beneath the BHSZ. Hydrate growth (and disassociation) within the HSZ is determined when the local methane concentration is greater (lower) than the equilibrium methane concentration. Beneath the BHSZ methane bubbles form instead of hydrate.

We model the freshening of pore fluids so that chlorine predictions can be compared against observations. A forthcoming paper will discuss improvements we are making to the model and provide full details of the transient model and its performance.

Methane sources

We model both in-situ biogenic methanogenesis and the influx of methane bearing fluids using the mass transfer equations of [12]. Global data of Sedimentation rate and TOC are sparse, so we use geographically invariant, parameterized *TOC* (as a function of water-depth and dissolved oxygen [34,35] and sedimentation rates, *sed* (a function of water-depth [36]) supplemented with observed data to specify the carbon available within the upper sediment column. The mass-transfer model of [11] is used to determine biogenic methane generation. An upward-directed fluid velocity is specified (as well as methane saturation). Parameters that cannot be specified over a global domain (for example, *rxn* and *velup*) are determined through parameter optimization (see Hydrate model evaluation)

Model coupling and boundary conditions

The geographic distribution of modeled bottom water conditions and water depth are first linearly interpolated to 250 year resolution for input into the Transient model. We use geothermal gradients that are geographically invariant as well as spatially interpolated from sea floor heat flow and sediment conductivity global database (in a way similar to [37]). Given the reliance on some geographically invariant boundary conditions, further levels of complexity, such as glacial isostatic adjustments and changes to sediment properties with time were not incorporated into the global model, although this capability exists. Whilst we recognize that these aspects may play an important role in hydrate formation and

stability we will wait until improved datasets or models are available with sufficient temporal and spatial resolution. We use a standard heat conductivity equation [47] for the propagation of thermal anomalies through the sediment column. Hydrostatic pressure anomalies are assumed to propagate instantaneously from the sea-floor through the sediment column. When grounded ice sheets encroach on the marine realm, a basal temperature of 0 °C and a hydrostatic pressure equivalent to the weight of overlying ice is assumed.

When applying the 1-D transient model to the global domain, the model is run for every GCM grid cell (within the passive-active margin specification) with isolated 1-D sediment columns. Vertical fluid flow is specified by active and passive margin-type, calibrated to Blake Ridge and Cascadia Margin sites. The initial down-column methane concentration is set to zero. Our methodology has similarities with other global studies [34,37]. Currently, changes in bottom water salinity are not transported through the sediment, although GCM data is available. Whilst sediment porosity plays an important role in the physics of hydrate formation, we currently rely upon fixed values rather than derivations from wet-sediment conductivity [37,38].

HYDRATE MODEL EVALUATION

We consider the well-studied Blake Ridge and Cascadia Margins, sites where multiple lines of evidence indicate the existence of hydrate. In line with previous model evaluations we have considered fixed modern boundary conditions (i.e. ones that do not change through the simulation). This allows model performance to be compared against other similar studies and to allow generalised boundary conditions to be determined for passive and active margin sites (interstitial fluid velocity, sediment porosity). We consider fully-saturated fluids bearing up vertically from beneath with interstitial velocity $U_f(z=L)$.

Blake Ridge, ODP Leg 164, Site 997

We investigate potential uncertainty and variability in sedimentation rate, Total Organic Carbon (*TOC*), geothermal gradient (*G*), Porosity (*P*), methanogenesis rate constant (*rxn*), and the interstitial velocity ($U_f(z=L)$) using the envelopes defined by Table 1. We evaluate these envelopes

using a Latin-hypercube sampled (LHS) series of 10,000 runs each of 10 Myr in duration. For each run we determine a skill score using a chi-squared fit against the observed chlorinity profile. The top 1% of runs that develop hydrate define a subset which we consider the most optimum.

BWT (deg-C)	2.5 - 3.5
G (K/m)	0.039 - 0.043
Rxn ($3 \times 10^{-13} \text{ s}^{-1}$)	0.1 - 3.0
Sed (cm/kyr)	15 - 22
TOC (wt %)	1.0 - 1.5
P(z=0)	0.67-0.75
$U_f(z=L)$ (mm/yr)	0 - 1

Table 1. Blake Ridge boundary conditions.

Initial runs using the range of *rxn* specified within Table 1 result in optimal configurations (typically $rxn=2.5-3 \times 10^{-13}$) that have unrealistic levels of hydrate saturation of pore-space (>7.5%) and high interstitial velocities that are not supported by observations. Figure 1 shows the distribution of hydrate profiles from the optimal subset.

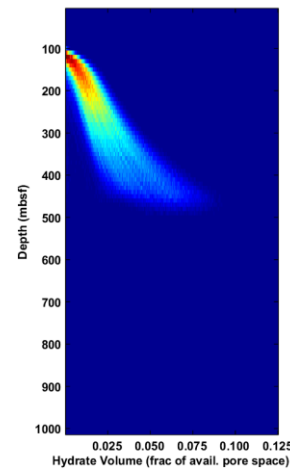


Figure 1. Distribution of hydrate occupancy of pore-space for the initial LHS run. The spread in BHSZ is a consequence of the envelopes of BWT and *G*.

A second run with *rxn* fixed at 0.15×10^{-14} (found by [37] to be more appropriate) resulted in more realistic hydrate volumes (at the cost of a reduction in chlorine fit). Modeled interstitial fluid velocity at the sediment-water interface ranged between 0.21 and 0.27 mm/yr, which is broadly consistent with Br^- and I^- concentrations [39] $^{37}\text{Cl}/^{35}\text{Cl}$ ratio studies [40] model fitting to Cl^- [12] of 0.20, 0.18, and 0.25 mm/yr respectively. Figure

2 shows the distribution of hydrate profiles from the optimal subset. Hydrates occupy 4.5 to 5.8% of pore space at the base of the HSZ, equivalent to an areal density of 434 and 588 kg/m² of hydrate. This pore space fraction is in good agreement with estimates from seismic velocity profiling [41], Pressure Core Sampling [42], and analysis of Chlorine profiles [43] with 5-7, 0-9, and 4-7 % respectively. Whilst our model is numerically equivalent to [12] given the same parameters, differences in results are likely a consequence of our optimisation method which leads to boundary conditions that differ to [12]. Our most optimum configuration, given Table 1, is $U_f(0)=0.20$ mm/yr, 5.4% pore space, and 519 kg/m² areal hydrate density.

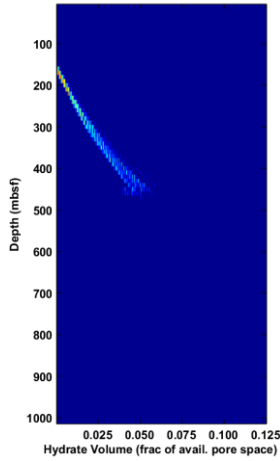


Figure 2. Subset of most optimized runs with rxn=0.15.

Cascadia Margins, ODP Leg 146, Site 889

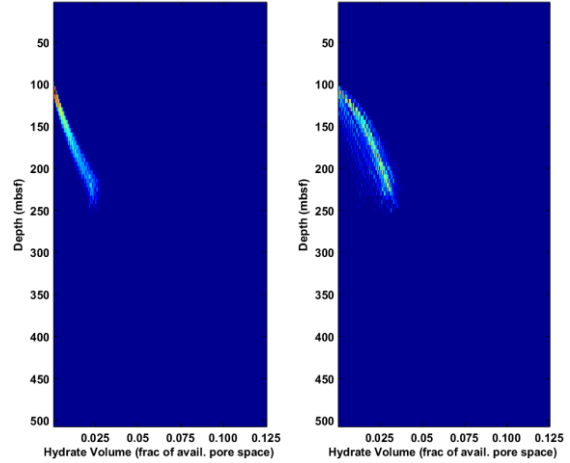
We follow the procedure as defined for Blake Ridge but use two sets of parameters that explore a system with fluid-only and a system of fluid and in-situ sources. Parameters are defined within Table 2. Depth profile of Chlorine from [44]

	Fluid-only	In-situ and fluid
BWT (deg-C)	2.7 – 4.0	2.7 – 4.0
G (K/m)	0.054 - 0.060	0.054 - 0.060
Rxn ($3 \times 10^{-13} \text{ s}^{-1}$)	0	0.1 - 3.0
Sed (cm/kyr)	25	25
TOC (wt %)	0	0 - 1.0
P(0)	0.55 - 0.65	0.55 - 0.65
$u_f(z)$ (mm/yr)	0 - 10	0 - 10

Table 2. Cascadia Margins boundary conditions.

Within a fluid-only system we find the optimal subset consists of a range in interstitial fluid velocities (at the sea-sediment/surface) of between

0.61 and 0.78 mm/yr with peak pore space saturation of 2.3 to 2.8%. This is higher than the peak 1% saturation measured by [45]. With a HOZ that begins at ~100 mbsf, hydrate areal densities of between 79.2 and 127.0 kg/m² are predicted. The most optimum parameter set $u_f(0)=0.62$ mm/yr, 2.5% pore space, and 105.5 kg/m² areal hydrate density. Optimal configurations are shown within Figure 3.



Figures 3 (left) and 4 (right) show the most optimal distributions of pore-space hydrate occupancy for the Fluid-only (left) and Fluid + in-situ sources (right).

Under the system with both in-situ source and influx of fluids we observe an improved fit to chlorine at the BHSZ compared to a fluid-only system. The optimal subset consists of fluid velocities between 0.29 and 0.39 mm/yr with peak pore space saturation of 1.5 to 3.8%. Areal hydrate densities of between 44.1 and 211 kg/m² are predicted. Figure 4 shows the hydrate profiles for the optimum subset. The most optimum parameter set is $u_f(0)=0.33$ mm/yr, 3.6% pore space, and 197 kg/m² areal hydrate density.

TRANSIENT MODELLING

Strategy and experiment design

Our Transient modeling strategy involves three stages, (1) Model intialisation in which we run with initial-state boundary condition until steady state is achieved, (2) Relaxation stage where we linearly interpolate bottom water condition and sea level from Pliocene to Glacial over a period of 1.5 Myr. (3) Glacial-cycle stage where we cycle conditions through n glacial cycles. This process is carried out at the resolution of the HadCM3 ocean

($1.25^\circ \times 1.25^\circ$) over a mask specifying continental margins (i.e. the passive-active margin mask of [48], or by a bathymetric cut-off)

We consider the mid-Pliocene warm period (mPWP) as a suitable initial boundary condition for a number of reasons. (1) It is the most recent geological time interval which represents an extended period of warmth (and hence shallow global HSZ) (2) Many marginal sediments are of Pliocene age. (3) The mPWP has boundary conditions (for example, surface topography, vegetation, ice sheet configuration) that are well-studied and so we have good confidence in specifying model boundary conditions (4) There is a significant database of geological proxies that allow us to evaluate our predicted climatologies (i.e PRISM3 ocean reconstruction [23]) (5) It is the earliest period that has been extensively studied with long-integration HadCM3 GCM runs, (6) The positions of the continents are similar to the present-day and so we do not require plate-rotation.

Blake Ridge run

We demonstrate the experiment design by modelling Blake Ridge using GCM modeled bottom water temperatures (Pliocene to pre-industrial), changing sea level, and parameters derived from the Hydrate model evaluation. Simulation results from a 20 pseudo-glacial cycle run are shown within Figure 5.

We see a complex interplay between the instantaneous changes in pressure and the lagged propagation of the temperature anomalies through the sediment column. Generally BHSZ minima are ~4 to 7 kyr behind coldest BWT. The calculated present-day BHSZ is deeper than observations, this is likely due to using a GCM modeled temperature (which slightly underestimate Blake Ridge conditions).

Modeling the response of the global HSZ and hydrate inventory to 100 kyr glacial cycles.

A series of steady-state (using fixed boundary conditions) and fully transient runs through pseudo-glacial cycles has been carried out and explored using a series of sensitivity experiments. These will be presented in future publications. We report on a study into the evolution of the global HSZ volume was conducted using the modelled

bottom water temperatures and sea-level reconstruction.

Assuming hydrates are restricted to the margins as defined by [48], shown within Figure 6, it is possible to calculate how the volume of the global HSZ changes through the glacial cycle.

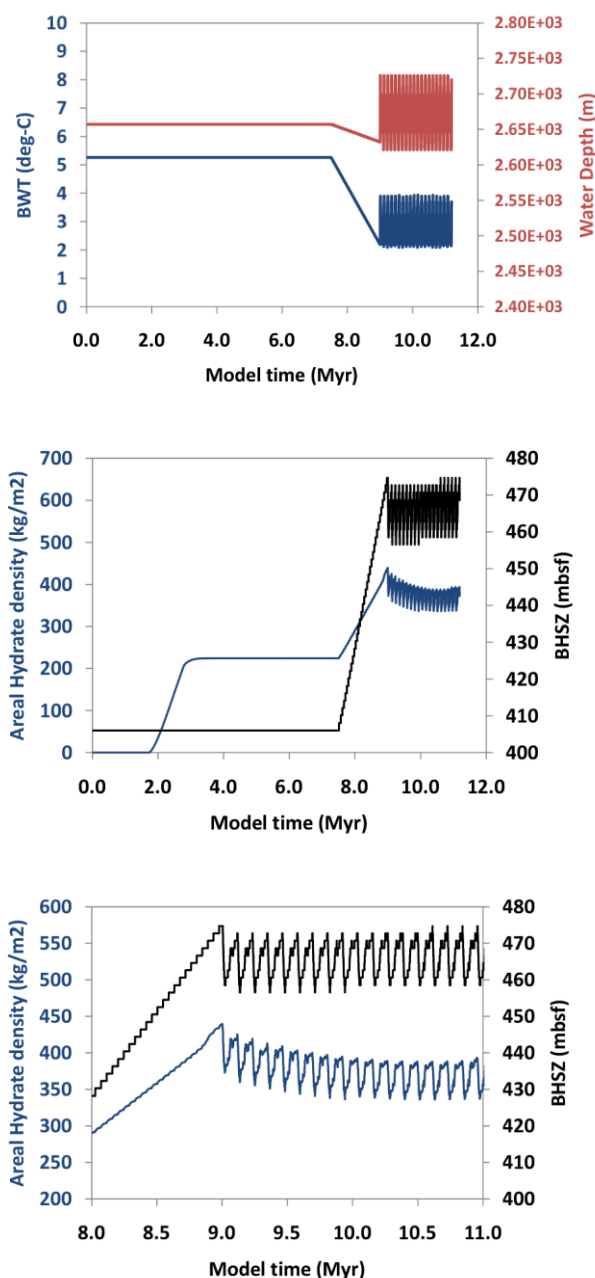


Figure 5. (Top) Bottom water temperature and water depth through the Blake Ridge simulation. (middle and bottom) Modelled hydrate stability zone base and areal hydrate density.

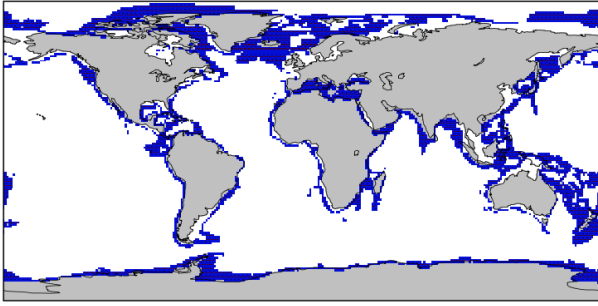


Figure 6. Mask of active and passive margins adapted from [48]

We find that during the mPWP the global volume of the HSZ is $14.6 \times 10^6 \text{ km}^3$ whilst during the last glacial cycle it ranges from between 15.9 and $16.2 \times 10^6 \text{ km}^3$ as shown within Figure 7 (bottom). Assuming an average porosity of 50% we obtain a potential volume of gas hydrate of between 7.95 and $8.10 \times 10^6 \text{ km}^3$, compared to $7.3 \times 10^6 \text{ km}^3$ for the mPWP. Given typical down-column hydrate profiles (i.e. Figures 2-4), these potential volumes are expected to greatly overestimate the global hydrate volume. Nevertheless, these values are similar to the predictions of [46] who calculated values for the present day of between 3.5 and $>12.5 \times 10^6 \text{ km}^3$ using a series of idealized margin cross sections integrated along the worlds margins. With a model resolution of 1.25° (approx. 140 and 100 km resolution at the equator and 45 degrees latitude respectively) and a global bathymetry binned into 20 discrete depths we expect to under-represent the dynamics of the HSZ in shallower waters (i.e. towards the shelf break), regions which may be more susceptible to changes in sea-level. The treatment of subsea permafrost is also omitted from this series of simulations and so shallow water arctic deposits are not currently represented. We plan to explore these within a future study.

The calculated evolution of the global HSZ volume reflects the complex interplay between ice-sheets (changes in sea-level) and bottom water conditions (responding to changes in ocean circulation and atmospheric composition etc). We are currently in the process of analyzing and conducting sensitivity studies of the global hydrate volume, using the Transient hydrate model at the full GCM ocean spatial resolution ($1.25^\circ \times 1.25^\circ$).

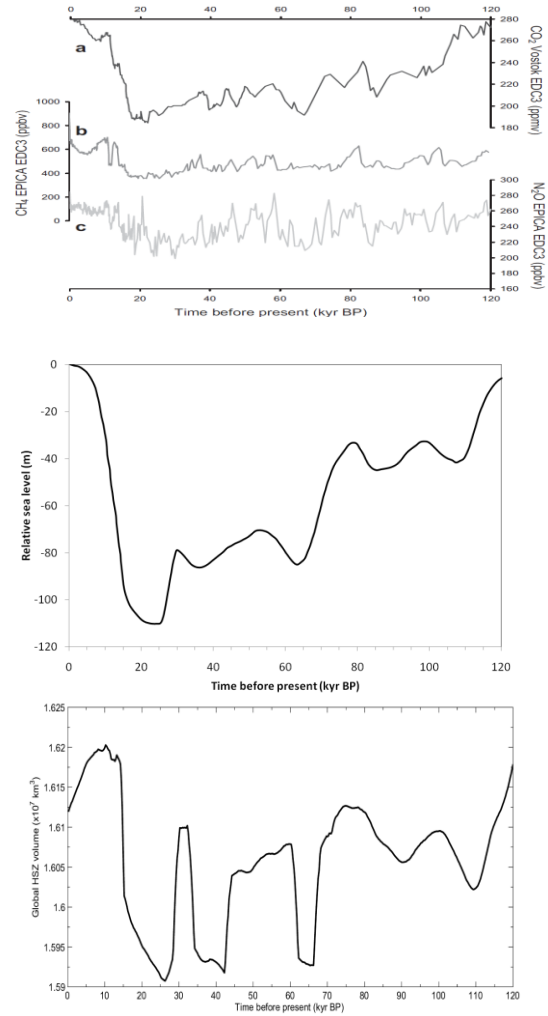


Figure 7. (top) the atmospheric composition, adapted from [25 and references therein] (middle) the eustatic glacial-equivalent sea-level from [31] (bottom) the integrated volume of the global HSZ given the margin specification of Figure 6 (assuming $G = 0.042 \text{ K/m}$ and a sediment thermal diffusivity of $10^{-6} \text{ m}^2/\text{s}$).

Summary and Significance of work

We have adapted and evaluated an existing hydrate model to accept evolving boundary conditions. A fully-coupled atmosphere-ocean GCM is used to derive initial (Pliocene) and glacial cycle (120 kyr BP to present) boundary conditions. We model the steady state inventory (using Pliocene boundary conditions) and model how this evolves through a series of pseudo-glacial cycles. We have presented aspects of our model evaluation and results of our calculation of evolution of the global HSZ volume. The full model evaluation and our calculations of the evolution of the global methane hydrate inventory will be presented within future publications. This

work, to the best of our knowledge, represents the first attempt to derive the evolution of the global methane hydrate inventory using an extensive dataset of long integration GCM runs as a boundary condition for a hydrate model.

Future work

Our goal will be to specify more realistic input fields. We plan to use Earth system models to better specify the boundary conditions required by the hydrate model (i.e. better representation of ocean carbon cycle, river routing schemes, sedimentation, glacial erosion and bottom water oxygen) and to incorporate glacial isostatic adjustments. We will use a sediment diagenesis model to couple the bottom water conditions and sediment supply to the upper sediment column. We have also developed more advanced physics packages which will be integrated into the model, including lateral-flows, improved thermodynamics and pore-scale physics. As model boundary conditions become better-specified so will the requirement for improved physics.

The HadCM3 run interval (min 1 kyr) does not capture potentially important Millennial-scale climate oscillations such as Dansgaard-Oeschger and Heinrich events cycles. However it is hoped that the larger-scale climatic signal is captured with some fidelity. Future work will utilize Transient FAMOUS GCM simulations of these millennial-scale events to better capture changing bottom water conditions.

REFERENCES

[1] Maslin, M., et al., *Gas hydrates: past and future geohazard?* Philosophical Transactions of the Royal Society A: Mathematical, Physical and Engineering Sciences, 2010. 368(1919): p. 2369-2393.

[2] Maclennan, J. and S.M. Jones, *Regional uplift, gas hydrate dissociation and the origins of the Paleocene-Eocene Thermal Maximum.* Earth and Planetary Science Letters, 2006. 245(1-2): p. 65-80.

[3] Dunkley Jones, T., et al., *A Palaeogene perspective on climate sensitivity and methane hydrate instability.* Philosophical Transactions of the Royal Society A: Mathematical, Physical and Engineering Sciences, 2010. 368(1919): p. 2395-2415.

[4] Kennett, J.P., et al., *Methane Hydrates in Quaternary Climate Change: The Clathrate Gun Hypothesis.* 2003, Washington D. C.: AGU.

[5] Nisbet, E.G., *The end of the ice age.* Canadian Journal of Earth Sciences, 1990. 27: p. 148-157.

[6] Paull, C.K., W. Ussler, and W.P. Dillon, *Is the extent of glaciation limited by marine gas hydrates?* Geophysical Research Letters, 1991. 18(3): p. 432-434.

[7] Kvenvolden, K.A., *Potential effects of gas hydrate on human welfare.* Proceedings of the National Academy of Sciences of the United States of America, 1999. 96(7): p. 3420-3426.

[8] McIver, R.D., *Role of naturally occurring gas hydrates in sediment transport.* American Association of Petroleum Geologist Bulletin, 1982. 66(6): p. 789-792.

[9] Henriot, J.-P. and J. Mienert, *Gas Hydrates: Relevance to world margin stability and climate change.* Special Publication of the Geological Society of London, 1998. 137.

[10] Bugge, T., S. Befring, and R.H. Belderson, *A giant three-stage submarine slide off Norway.* Geo-Marine Letters, 1987. 7: p. 191-198.

[11] Kayen, R.E. and H.J. Lee, *Pleistocene slope instability of gas hydrate-laden sediment on the Beaufort sea margin.* Marine Geotechnology, 1991. 10(1): p. 125 - 141.

[12] Davie, M.K. and B.A. Buffett, *A numerical model for the formation of gas hydrate below the seafloor.* Journal of Geophysical Research, 2001. 106: p. 497-514.

[13] Davie, M.K., *Numerical models for the formation of marine gas hydrates: Constraints on methane supply from a comparison of observations and numerical models,* in Department of Earth and Ocean Sciences. 2002, The University of British Columbia.

[14] Gregory, J.M. and J.F.B. Mitchell, *The climate response to CO₂ of the Hadley Center coupled AOGCM with and without flux adjustments.* Geophysical Research Letters, 1997. 24: p. 1943-1946.

[15] Gordon, C., et al., *The simulation of SST, sea ice extents and ocean heat transports in a version of the Hadley Centre coupled model without flux adjustments.* Climate Dynamics, 2000. 16: p. 147-168.

[16] Megann, A.P., et al., *The Sensitivity of a Coupled Climate Model to Its Ocean Component.* Journal of Climate, 2010. 23: p. 5126-5150.

[17] Randall, D.A. and e. al, *Climate Models and Their Evaluation, in The Physical Basis of Climate Change. Contribution of Working Group I to the Fourth Assessment Report of the IPCC,* S. Solomon and e. al., Editors. 2007, Cambridge University Press: Cambridge and New York.

[18] Gladstone, R.M., et al., *Mid-Holocene NAO: A PMIP2 model intercomparison.* Geophysical Research Letters, 2005. 32(L16707).

[19] Hewitt, C.D., et al., *A coupled model study of the last glacial maximum: Was part of the North Atlantic relatively warm?* Geophysical Research Letters, 2001. 28(8): p. 1571-1574.

[20] Brown, J., et al., *Modelling mid-Holocene tropical climate and ENSO variability towards constraining*

predictions of future climate change with palaeo-data. Climate Dynamics, 2008. 30(1): p. 19-36.

[21] Haywood, A.M. and P.J. Valdes, *Modelling Pliocene warmth: contribution of atmosphere, oceans and cryosphere*. Earth and Planetary Science Letters, 2004. 218(3-4): p. 363-377.

[22] Bonham, S.G., et al., *El Nino-Southern Oscillation, Pliocene climate and equifinality*, Philosophical Transactions of the Royal Society, A., 2009. 367, p.127-156.

[23] Dowsett, H. J., et al., *Sea Surface Temperatures of the Mid-Piacenzian Warm Period: A Comparison of PRISM3 and HadCM3*, Palaeo-3, (in press)

[24] Lunt, D.J., et al., *CO₂ driven ocean circulation changes as an amplifier of Paleocene-Eocene thermal maximum hydrate destabilisation*. Geology, 2010. 38: p. 875-878.

[25] Singarayer, J.S. and P.J. Valdes, *High-latitude climate sensitivity to ice-sheet forcing over the last 120 kyr*. Quaternary Science Reviews, 2010. 29 (1-2): p. 43-55.

[26] Berger, A. and M.F. Loutre, *Insolation values for the climate of the last 10 million years*. Quaternary Science Reviews, 1991. 10: p. 297-317.

[27] Petit, J.R., et al., *Climate and atmospheric history of the past 420 000 years from the Vostok Ice Core, Antarctica*. Nature, 1999. 399: p. 429-436.

[28] Loulergue, L., et al., *Orbital and millennial-scale features of atmospheric CO₂ over the past 800,000 years*. Nature, 2008. 453: p. 383-386.

[29] Spahni, R., et al., *Variations on atmospheric methane and nitrous oxide during the last 650 000 years from Antarctic ice cores*. Science, 2005. 310: p. 1317-1321.

[30] Peltier, W.R., *Global glacial isostasy and the surface of the ice-age earth: The ICE-5G (VM2) Model and GRACE*. Annual Review Earth and Planetary Science, 2004. 32: p. 111-149.

[31] Peltier, W.R. and R.G. Fairbanks, *Global glacial ice volume and Last Glacial Maximum duration from an extended Barbados sea level record*. Quaternary Science Reviews, 2006. 25(23-24): p. 3322-3337.

[32] Martinsen, D.G., et al., *Age dating and orbital theory of the ice ages: development of a high resolution 0-300,000 year chronostratigraphy*. Quaternary Research, 1987. 27: p. 1-30.

[33] Lamarque, J.-F., *Estimating the potential for methane clathrate instability in the 1%-CO₂ IPCC AR-4 simulations*. Geophysical Research Letters, 2008. 35(19) p. L19806.

[34] Buffett, B. and D. Archer, *Global inventory of methane clathrate: sensitivity to changes in the deep ocean*. Earth and Planetary Science Letters, 2004. 227(3-4): p. 185-199.

[35] Archer, D.E., J.L. Morford, and S.R. Emerson, *A model of suboxic sedimentary diagenesis suitable for automatic tuning and gridded global domains*. Global Biogeochemical Cycles, 2002. 16.

[36] Middelburg, J.J., K. Soetaer, and P.M.J. Herman, *Empirical relationships for use in global diagenetic models*. Deep-Sea Research I, 1997. 44(2): p. 327-344.

[37] Klauda, J.B. and S.I. Sandler, *Global Distribution of Methane Hydrate in Ocean Sediment*. Energy and Fuels, 2005. 19(2): p. 459-470.

[38] Klauda, J.B. and S.I. Sandler, *Predictions of gas hydrate phase equilibria and amounts in natural sediment porous media*. Marine and Petroleum Geology, 2003. 20(5): p. 459-470.

[39] Egeberg, P.K. and G.R. Dickens, *Thermodynamic and pore water halogen constraints on gas hydrate distribution at ODP Site 997 (Blake Ridge)*. Chemical Geology, 1999. 153(1-4): p. 53-79.

[40] Hesse, R., et al., *Stable isotope studies (Cl, O and H) of interstitial waters from Site 997, Blake Ridge gas hydrate field, West Atlantic*, in Proc. Ocean Drill. Program Sci. Results, C.K. Paull, et al., Eds.. 2000.

[41] Holbrook, W.S., et al., *Methane Hydrate and Free Gas on the Blake Ridge from Vertical Seismic Profiling*. Science, 1996. 273(5283): p. 1840-1843.

[42] Dickens, G.R., C.K. Paull, and P. Wallace, *Direct measurement of in situ methane quantities in a large gas-hydrate reservoir*. Nature, 1997. 385: p. 426-428.

[43] Egeberg, P.K. and G.R. Dickens, *Thermodynamic and pore water halogen constraints on gas hydrate distribution at ODP Site 997 (Blake Ridge)*. Chemical Geology, 1999. 153(1-4): p. 53-79.

[44] Westbrook, G.K., et al., *Sites 889 and 890*, in Proceedings of the Ocean Drilling Program, Initial Reports. 1994.

[45] Milkov, A.V., et al., *In situ methane concentrations at Hydrate Ridge, offshore Oregon: New constraints on the global gas hydrate inventory from an active margin*. Geological Society of America, 2003: p. 803-836.

[46] Dickens, G.R., *The potential volume of oceanic methane hydrates with variable external conditions*. Organic Geochemistry, 2001. 32(10): p. 1179-1193.

[47] A. N. Tikhonov and A. A. Samarskii, *Equations of Mathematical Physics* (Dover Publications, 1990) 784

[48] Archer, D., B. Buffett, and V. Brovkin, *Ocean methane hydrates as a slow tipping point in the global carbon cycle*. Proceedings of the National Academy of Sciences of the United States of America, 2009. 106(49): p. 20596-20601.

ACKNOWLEDGEMENTS

I (SH) would like to thank Ron Kahana (Bristol now UKMO) for discussions, Bruce Buffett and David Archer for supplying the original models. This project was funded under the UK Natural Environment Research Council (NERC) Grant No. NE/F021941/1.